JOURNAL OF APPLIED PHYSICS 116, 063506 (2014)

Tunable band gaps in bio-inspired periodic composites with nacre-like microstructure

Yanyu Chen and Lifeng Wang[a)]
Department of Mechanical Engineering, State University of New York at Stony Brook, Stony Brook, New York 11794, USA

(Received 29 March 2014; accepted 29 July 2014; published online 12 August 2014)

Periodic composite materials have many promising applications due to their unique ability to control the propagation of waves. Here, we report the existence and frequency tunability of complete elastic wave band gaps in bio-inspired periodic composites with nacre-like, brick-and-mortar microstructure. Numerical results show that complete band gaps in these periodic composites derive from local resonances or Bragg scattering, depending on the lattice angle and the volume fraction of each phase in the composites. The investigation of elastic wave propagation in finite periodic composites validates the simulated complete band gaps and further reveals the mechanisms leading to complete band gaps. Moreover, our results indicate that the topological arrangement of the mineral platelets and changes of material properties can be utilized to tune the evolution of complete band gaps. Our finding provides new opportunities to design mechanically robust periodic composite materials for wave absorption under hostile environments, such as for deep water applications. © *2014 AIP Publishing LLC*. [http://dx.doi.org/10.1063/1.4892624]

I. INTRODUCTION

Periodic composite materials with spatially modulated elastic constants and mass densities have attracted much interest owing to their capability to manipulate the propagation of mechanical waves.[1–4] Interesting phenomenon arises in band structures, known as complete band gaps (CBGs)—frequency ranges within which mechanical waves are totally reflected by the structure irrespective of the incident angle or their propagation is prohibited if the mechanical wave is generated inside of the structure. This fundamental property promises many novel applications, such as wave filtering,[5–7] waveguiding,[8–10] and energy harvesting.[11–13]

The formation of CBGs is led by two mechanisms, Bragg scattering and local resonances.[14,15] Bragg scattering is based on diffraction and it arises when the relevant wavelengths of mechanical waves are on the order of the periodicity of the composites. Periodicity, topology, and the contrast in elastic constants and densities of constituent materials are all of great concern.[14] Bragg-type CBGs has been reported in two-dimensional (2D) and three-dimensional (3D) periodic composites with different combinations of constituent materials and different lattice symmetries.[16–19] In addition, topology-optimization method has been implemented to maximize the relative width of Bragg-type CBGs in 2D composites.[20] Interestingly, recent studies demonstrate that large deformation can be used to tune the evolution of Bragg-type CBGs in 2D and 3D soft periodic solids.[21,22] Local resonances can also give rise to the formation of CBGs where the frequency is dictated by the frequency of the resonance. For example, the frequency of a resonance gap can be two orders of magnitude lower than those resulted from Bragg scattering.[23] This phenomenon is attributed to the insertion of a relatively soft material and hence the frequency of a resonance CBG is independent of periodicity and symmetry in general.[14,24,25] Although periodic composites have been extensively investigated, it is still a challenge to design and fabricate mechanically robust periodic composites with well-defined topology and desired CBGs.

Recently, hard biological materials are of great interest because of their remarkable mechanical performance that cannot be readily achieved in man-made composites. For instance, fish scales, lobster cuticles, and crab claws have been found to possess extraordinary capability to resist dynamic loading.[26–30] In addition, the highly ordered brick-and-mortar arrangement of hard inorganic and soft organic materials in seashell nacre and bones enables unusual combinations of stiffness, strength, impact resistance, and toughness.[31–37] The structure-function harmony in these biological materials suggests that there may be a strong correlation between the resistance of mechanical waves and the underlying microstructures and also provides the opportunity to enhance multi-functions of the bio-inspired composite materials.

In this work, we specifically focus on investigating elastic wave propagation in periodic composites with 2D nacre-like, brick-and-mortar microstructure using finite element analysis (FEA). Firstly, the existence of CBG and the mechanisms of CBG formation in the considered periodic composites are investigated. Then, we validate the simulated CBGs and further reveal the mechanisms of CBG formation through analyzing elastic wave propagation in the periodic composites consisting of a finite number of unit cells. Finally, the effects of topological arrangement of the mineral platelets and the material properties of organic matrix on the frequency tunability of CBGs are studied. The results of this

[a)]Author to whom correspondence should be addressed. Electronic mail: Lifeng.wang@stonybrook.edu. Telephone: 631-632-1182.

work will provide new avenues to design mechanically robust metamaterials while having integrated wave filtering property.

II. NUMERICAL MODELING

A. Characterization of the unit cell

The considered periodic composites with nacre-like microstructure consist of multilayered staggered mineral platelets embedded in the organic matrix, as schematically illustrated in Fig. 1(a). The periodicity of the 2D microstructure is characterized by a rhombic lattice with vectors $\mathbf{a_1} = \mathbf{a_2} = [(L+d)/2,\ \tan\alpha\cdot(L+\mathrm{d})/2]$, where L is the length of the mineral platelet, d is the thickness of the organic matrix along x direction, and α is the lattice angle. (see Fig. 1(b)). The volume fraction (V_f) of the mineral platelets is characterized as

$$V_f = \frac{2Lh}{(L+d)^2 \cdot \tan\alpha}, \tag{1}$$

where h is the height of the mineral platelets. Note that the manner of defining volume fraction using the lattice angle enables us to distinguish the First Brillouin zone (FBZ) for the unit cell with different lattice angles and hence provides a convenient way to parametrically study the effect of geometric features on the evolution of CBGs.

B. Governing equation and material behavior

The governing equation of elastic wave propagation in inhomogeneous medium is given by

$$\nabla \cdot \boldsymbol{\sigma}(\mathbf{u}) = -\rho\omega^2\mathbf{u}, \tag{2}$$

where $\boldsymbol{\sigma}$ is the Cauchy's stress tensor, $\mathbf{u}$ is the displacement vector, ω is the angular frequency, and ρ is the mass density of the constituent material.

The constitutive relations of elasticity among the stress, the strain, and the displacement fields for a linear elastic material are given by

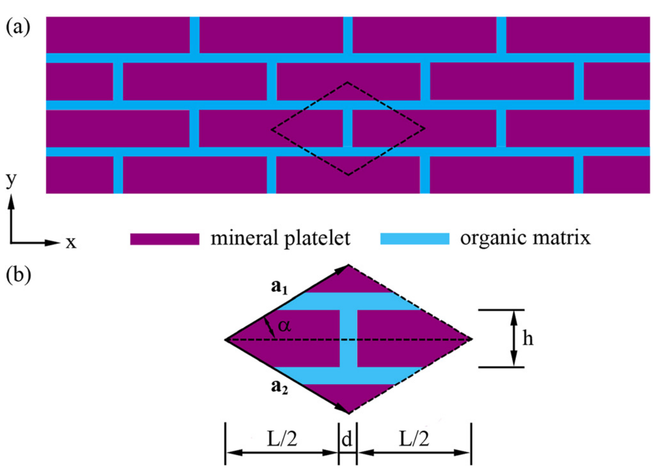

FIG. 1. (a) Schematic illustration of 2D nacre-like periodic composites consisting of mineral platelets and organic matrix. (b) 2D unit cell. L is the length of the mineral platelets; d is the thickness of the organic matrix along x direction and α is the lattice angle.

$$\boldsymbol{\sigma} = \mathbf{C} : \boldsymbol{\varepsilon} \tag{3}$$

$$\boldsymbol{\varepsilon} = \frac{1}{2}[(\nabla\mathbf{u})^T + \nabla\mathbf{u}], \tag{4}$$

where $\mathbf{C}$ is the 4th order elasticity tensor, $\boldsymbol{\varepsilon}$ is the strain tensor.

C. Boundary condition using Bloch's theorem

The characteristic of elastic wave propagation in periodic composites can be captured by studying the unit cell according to Bloch's theorem. In this case, Floquet periodic boundary conditions are applied at all the boundaries of the unit cell such that[38]

$$\mathbf{u}_i(\mathbf{r}+\mathbf{R}) = e^{i\mathbf{k}\cdot\mathbf{R}}\mathbf{u}_i(\mathbf{r}), \tag{5}$$

where $\mathbf{r}$ is the location vector, $\mathbf{R}$ is the lattice translation vector, and $\mathbf{k}$ is the wave vector.

The governing equation (2) combining with the boundary condition, Eq. (5), leads to the standard eigenvalue problem,

$$(\mathbf{K}\text{–}\omega^2\mathbf{M})\mathbf{u} = 0, \tag{6}$$

where $\mathbf{K}$ and $\mathbf{M}$ are the global stiffness and mass matrices assembled using standard FEA procedure.

The unit cell is discretized using 6-node triangular elements. Equation (6) is solved by imposing two components of wave vectors and hence yields the corresponding eigenfrequencies. The band structures are obtained by scanning of wave vectors in the FBZ. The FBZs of the unit cells with different ranges of lattice angles are constructed by calculating the associated reciprocal lattices, as illustrated in Fig. 2.

III. RESULTS AND DISCUSSION

The mineral platelets and the organic matrix are assumed to be linear elastic, homogeneous, and isotropic. The length of each mineral platelet is $L = 10\,\mu$m and the thickness of the organic matrix along x direction is $d = L/50 = 0.2\,\mu$m, which are similar to the values reported in nacre.[39–41] The material properties of the mineral platelets and the organic matrix are assigned as follows unless otherwise specified: for the mineral platelets, Young's modulus $E_m = 100$ GPa, density $\rho_m = 2950\,\mathrm{kg/m^3}$, and Poisson's ratio $\nu_m = 0.30$; for the organic matrix, Young's modulus $E_o = 20$ MPa, density $\rho_o = 1350\,\mathrm{kg/m^3}$, and Poisson's ratio $\nu_o = 0.30$.

A. Existence of CBG and mechanism of CBG formation

The band structures of the unit cells with different lattice angles are constructed in the corresponding FBZs to examine the existence of CBG in the considered composites. The volume fraction of the mineral platelets in each unit cell is set as 0.90 for comparison purposes. Band structures of the unit cells with lattice angles $\alpha = 10°\sim75°$ are shown in Fig. 3. Multiple CBGs arise in the band structures of the unit cells with lattice angles $\alpha = 10°\sim30°$. The frequency range of the widest CBG is $\omega = 162\sim200$ MHz for $\alpha = 10°$,

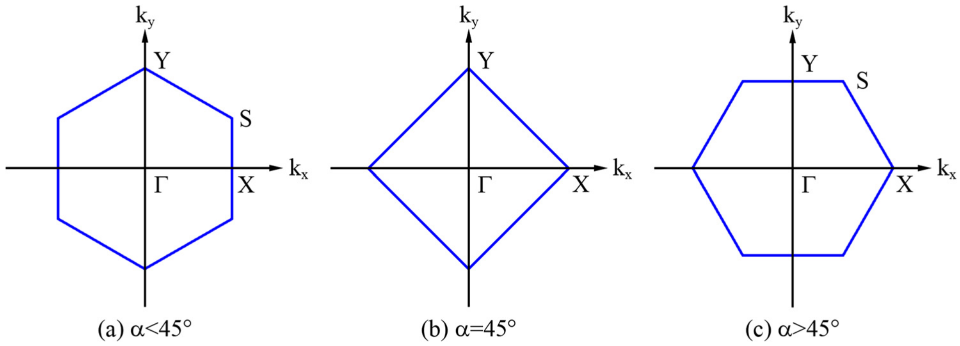

FIG. 2. The first Brillouin zones for the periodic composites with different ranges of lattice angles. (a) $\alpha<45°$, $\Gamma=(0,0)$, $X=\left(\frac{2\pi}{(L+d)},0\right)$, $S=\left(\frac{2\pi}{(L+d)},\frac{\pi}{(L+d)\cdot\tan\alpha}-\frac{\pi\cdot\tan\alpha}{(L+d)}\right)$, $Y=\left(0,\frac{\pi}{(L+d)\cdot\tan\alpha}+\frac{\pi\cdot\tan\alpha}{(L+d)}\right)$. (b) $\alpha=45°$, $\Gamma=(0,0)$, $X=\left(\frac{2\pi}{(L+d)},0\right)$, $Y=\left(0,\frac{2\pi}{(L+d)}\right)$ and (c) $\alpha>45°$, $\Gamma=(0,0)$, $X=\left(\frac{\pi}{(L+d)}+\frac{\pi}{(L+d)\cdot\tan^2\alpha},0\right)$, $S=\left(\frac{\pi}{(L+d)}-\frac{\pi}{(L+d)\cdot\tan^2\alpha},\frac{2\pi}{(L+d)\cdot\tan\alpha}\right)$, $Y=\left(0,\frac{2\pi}{(L+d)\cdot\tan\alpha}\right)$.

$\omega=105\sim180$ MHz for $\alpha=15°$, $\omega=38\sim133$ MHz for $\alpha=30°$. In contrast, only one CBG exists in each band structure of the unit cell when the lattice angle increases to $\alpha=45°\sim75°$. These results suggest the existence of CBGs in the periodic composites with nacre-like microstructure and also indicate that the geometric feature of the unit cell, i.e., the lattice angle, is significantly associated with the evolution of CBGs.

To reveal the mechanism of CBGs formation in the considered composites, band structure of the unit cell with lattice angle $\alpha=15°$ (Fig. 3(b)) is further discussed. The very flat bands are observed in the band structure and correspond to localized modes. The eigenmodes of the unit cells are plotted at given points (Point A and B) on the flat bands, as shown in Figs. 4(a) and 4(b). Evidently, the total displacement is almost concentrated in the organic matrix, indicating that the local resonances arise in the soft phase. Therefore, the formation of the CBG bounded by the flat bands is derived from locally resonant effects. However, the first CBG in the band structure is bounded by two normal bands and hence can be termed as a Bragg-type CBG, which is further supported by the corresponding eigenmodes at points C and D (Figs. 4(c) and 4(d)).

B. Elastic wave propagation in finite periodic composites

Now we investigate the behavior of elastic wave propagation in the periodic composites consisting of a finite number of unit cells. The goal of this analysis is, on the one hand, to validate the simulated CBGs by calculating the transmission coefficient of elastic wave propagation, and on the other hand, to further reveal the mechanisms of CBGs formation by observing the deformation behavior of the periodic composites. The periodic composite under investigation consists of an assembly of 4×8 unit cells sandwiched by two homogeneous parts of the organic matrix, as illustrated in Fig. 5(a). The volume fraction of mineral platelets is $V_f=0.90$ and the lattice angle is α=15° in the unit cell. To determine the transmission coefficient along YΓ direction,

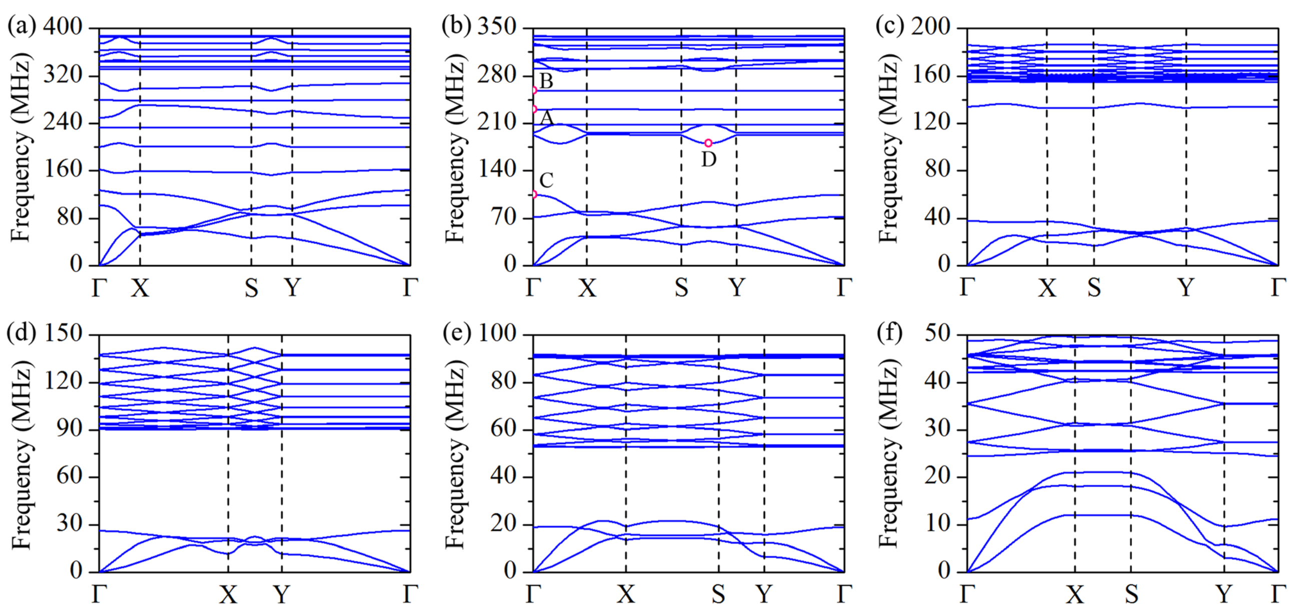

FIG. 3. Band structures of the unit cells with different lattice angles. (a) α=10°, (b) α=15°, (c) α=30°, (d) α=45°, (e) α=60° and (f) α=75°. The volume fraction of the mineral platelets is $V_f=0.90$.

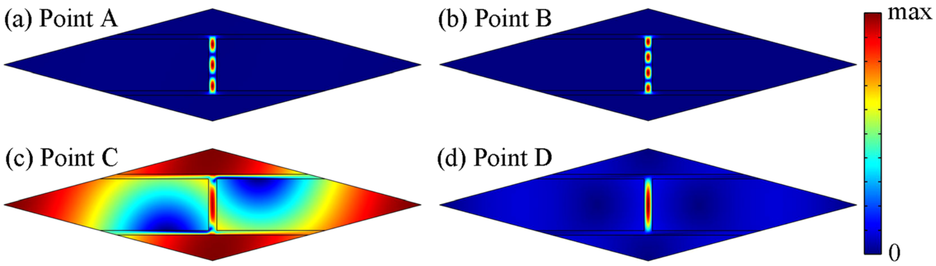

FIG. 4. Eigenmodes of the composites at the representative points in the band structure in Fig. (3). The color scale indicates the amplitude of total displacement.

an incident elastic wave along y direction is modeled by applying harmonic displacements with an amplitude of $u_0 = 0$ and $v_0 = 10\,\text{nm}$ in the x and y direction, respectively, at line S. Perfectly matched layers (PMLs) are applied at the two ends of the homogeneous part to prevent reflections by the scattering waves from the domain boundaries.[42] In addition, periodic boundary conditions are applied along the left and right edges of the considered composite. The transmission coefficient is defined as $\phi = 20\log[(|u|+|v|)/(|u_0|+|v_0|)]$, where u and v are horizontal and vertical displacements collected along the interface between PML and homogeneous part on the bottom side.

The frequency domain analysis sweeping from 0 to 350 MHz is performed and the simulated transmission coefficient as a function of frequency is plotted in Fig. 5(c). Strong attenuation zones can be observed in the transmission spectrum, which agree well with the corresponding partial band gaps along YΓ direction in the band structure (Fig. 5(b)). This confirms that the simulated CBGs in the band structure using Bloch theorem is reliable and also demonstrates the potential application of finite periodic composite as elastic wave filters.

To gain further insight into the mechanism of CBGs formation, we present in Fig. 6 the displacement fields of the composite at excitation frequencies below, within and above the CBGs. Figs. 6(a) and 6(b) show the horizontal and vertical displacement fields of the finite periodic composite at the frequency of 30MHz, which is below the first CBG. The incident elastic wave is partly reflected and partly passes through the periodic composite. Similar trend holds for the composite with incident wave frequency above the fourth CBG (Figs. 6(g)–6(h)). In contrast, the incident elastic wave is almost totally reflected and confined in the top homogeneous part when the frequency of the incident wave (130 MHz) lies within the first CBG (Figs. 6(c) and 6(d)). This phenomenon is consistent with what have been experimentally observed in a periodic array of pillars when the frequency of incident surface elastic wave lies in a Bragg-type band gap.[15] When the frequency of the incident wave lies in the third CBG, as shown in Figs. 6(e) and 6(f), the vertical displacement is localized in the organic matrix among the first mineral layer and the amplitude is amplified to 44.7 nm, indicating that locally resonant effect plays a role in wave absorption. These results provide direct support to our previous identification of the Bragg-type and locally resonant CBGs in the same periodic composite. It also demonstrates that two mechanisms can be achieved simultaneously to maximize CBGs in the same composite.

C. Effect of topological arrangement of mineral platelets

To understand the effect of topological arrangement of mineral platelets on the evolution of CBGs, two geometric parameters, the volume fraction and the lattice angle, are chosen to perform a parametric study. The effect of volume fraction on the evolution of CBGs for the unit cells with different lattice angles is shown in Figs. 7(a)–7(e). For the unit cell with a lattice angle $\alpha = 10^\circ$, three CBGs are observed and the width of these CBGs increases as the volume fraction increases from 0.50 to 0.80. When the volume fraction continues increasing, the width of the first two CBGs tends to

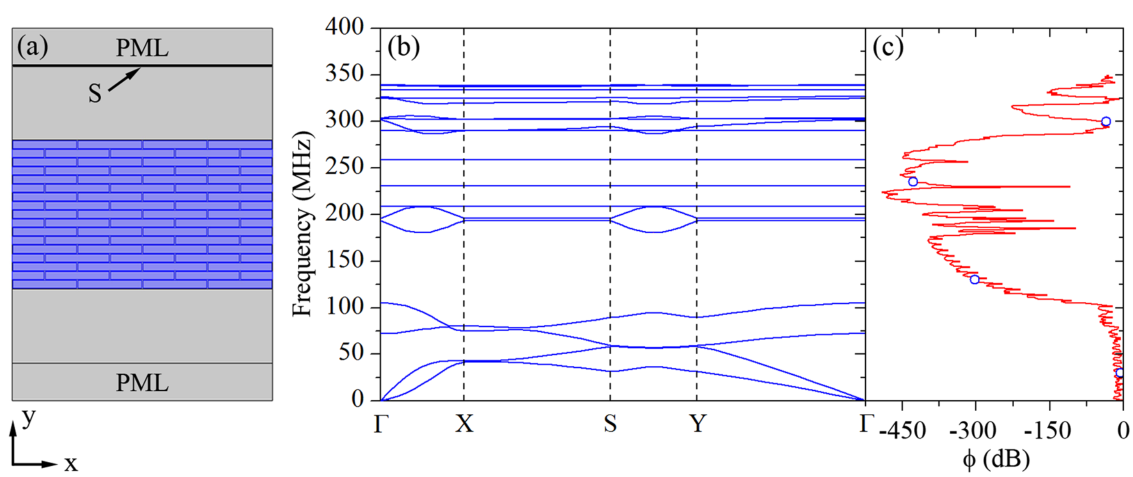

FIG. 5. (a) FEA model of the finite periodic composite consisting of 4×8 unit cells sandwiched by two homogeneous parts, where $\alpha = 15^\circ$ and $V_f = 0.90$. (b) The corresponding band structure and (c) the transmission coefficient along YΓ direction.

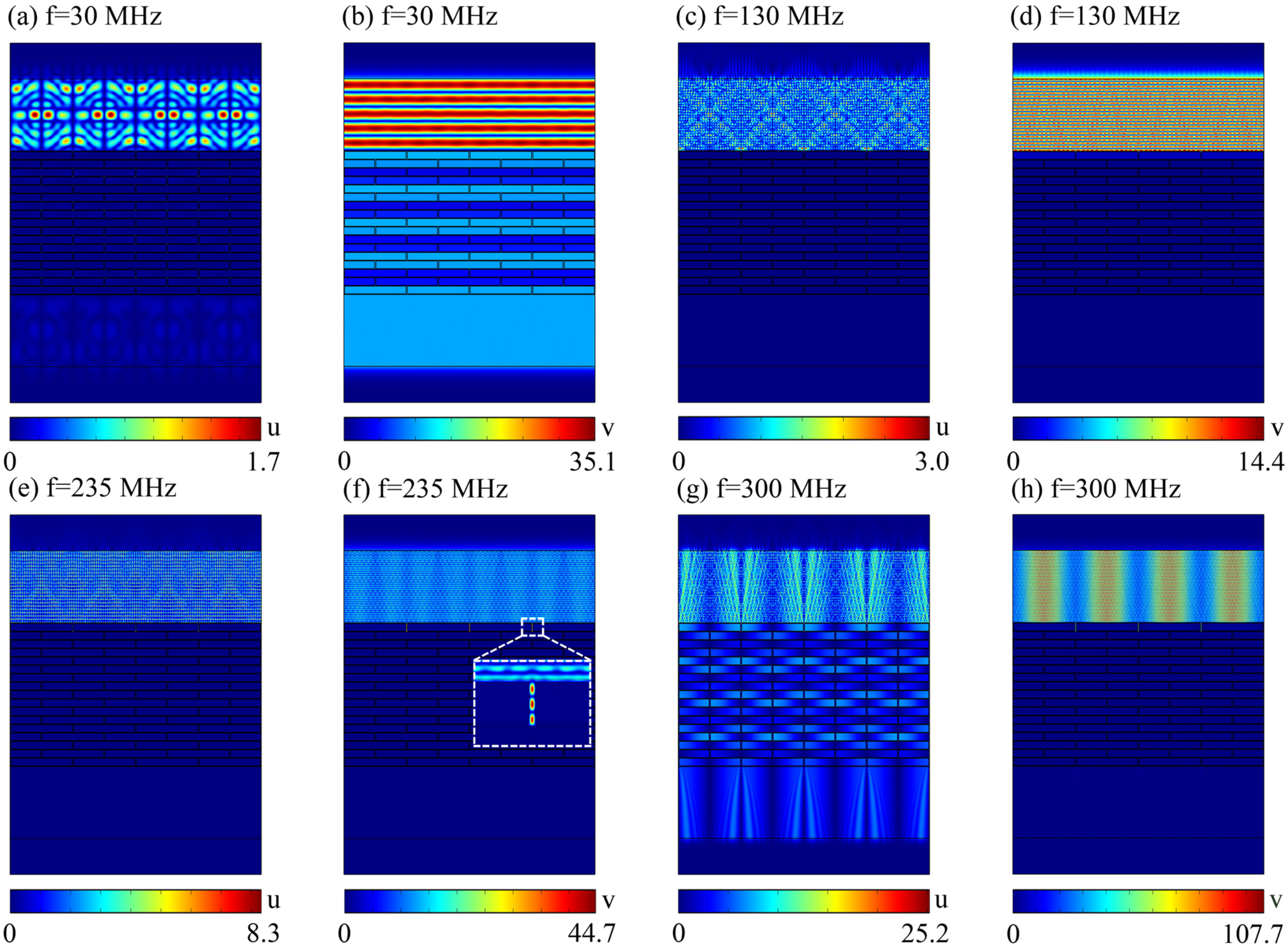

FIG. 6. Displacement field (nm) for elastic wave propagation in the considered periodic composite with excitation frequencies (a)–(b) 30 MHz, below the first CBG, (c)–(d) 130 MHz, within the first CBG, (e)–(f) 235 MHz, within the third CBG, and (g)–(h) 300 MHz, above the fourth CBG.

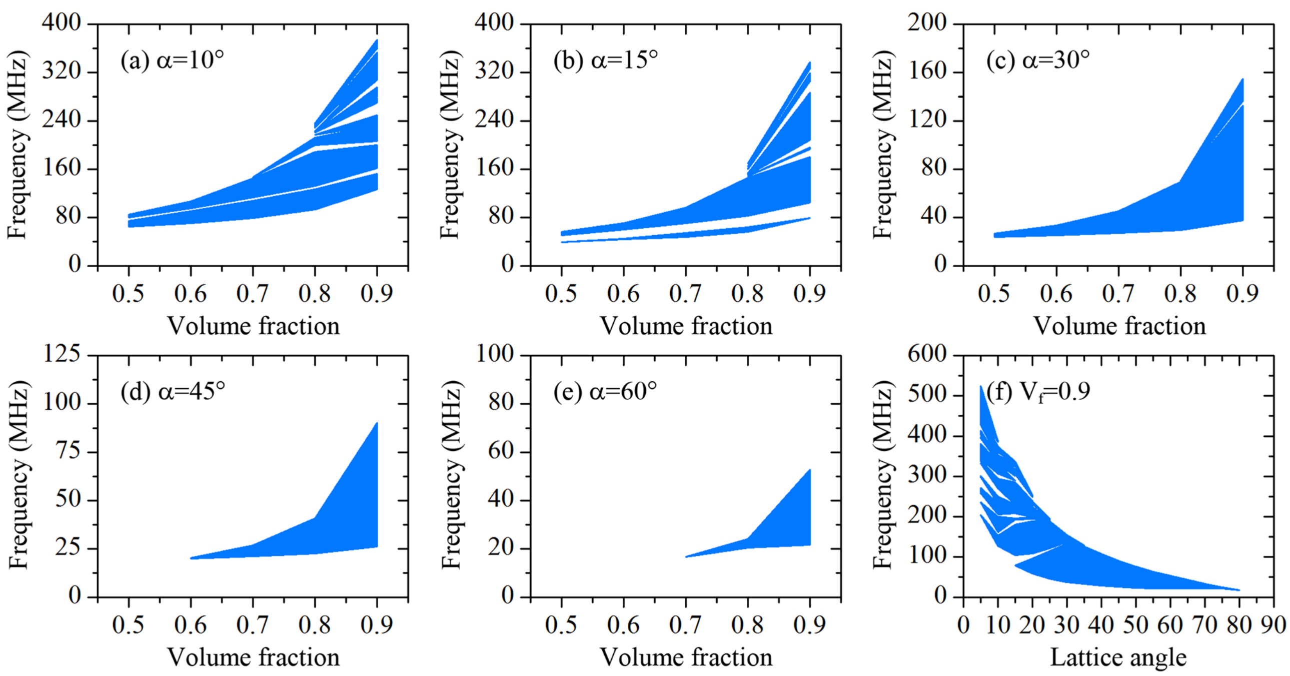

FIG. 7. Evolution of CBGs as a function of the volume fraction of the mineral platelets with different lattice angles. (a) α=10°, (b) α=15°, (c) α=30°, (d) α=45°, and (e) α=60°. (f) Evolution of CBGs as a function of the lattice angle, where $V_f = 0.90$.

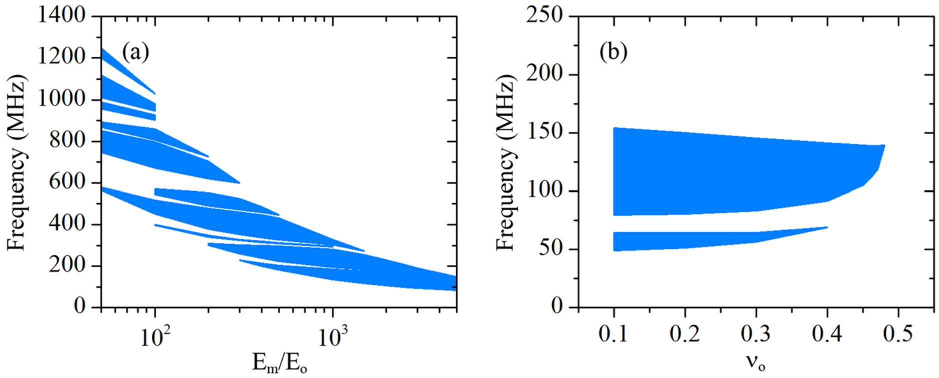

FIG. 8. Evolution of CBGs as a function of elastic constants, where $\alpha=15°$ and $V_f=0.80$. (a) Young's modulus ratio and (b) Poisson's ratio of the organic matrix.

shrink and several new CBGs arise. It shows that the maximum width of the first two CBGs is achieved at an intermediate volume fraction and these CBGs tend to close when the volume fraction is relatively high. This phenomenon is consistent with those have been observed in other 2D and 3D periodic composites, in which the CBGs are induced by Bragg scattering.[24,43] This behavior still exists for the first CBG of the unit cell with $\alpha = 15°$. However, the width of the rest CBGs enlarges and shifts towards higher frequency range as the volume fraction increases. The maximum widths of these CBGs are observed at the volume fraction of 0.90. For the unit cell with lattice angle $\alpha = 30° \sim 60°$, the maximum width of CBGs are all achieved at the volume fraction of 0.90. The only difference between these CBGs is that the CBGs open at larger volume fraction for larger lattice angle. These results indicate that the width of CBGs is governed by the volume fraction and hence can be tuned by tailoring the volume fraction for the unit cell with a given lattice angle.

The effect of lattice angle on the evolution of CBGs is presented in Fig. 7(f). The volume fraction of the mineral platelets is set as 0.90, where the periodic composite exhibits largest CBGs when the lattice angle is above 10°. The CBGs shift towards lower frequency range as the lattice angle increases. Two wide CBGs are observed for the unit cell with lattice angle $\alpha = 15° \sim 35°$. Specifically, the maximum width of the first CBG is 95.03 MHz with a lattice angle of 30° and the maximum width of second CBG is 80.06 MHz with a lattice angle of 20°. Moreover, the relative width of CBGs, which is defined as the ratio between gap width and the midgap location, in the unit cell with a lattice angle of 30° is 1.1, which is larger than those have been reported in other 2D and 3D periodic composites.[16,18,44]

These results indicate that the volume fraction of the mineral platelets and the lattice angle are two important geometric parameters governing the evolution of CBGs and also indicate that we can achieve desired CBGs in the periodic composites with optimal design.

D. Effect of material properties

It has been demonstrated that the contrast in elastic constants, wave velocities and densities of constituent materials is vital for the width and location of CBGs.[44] The contrast in elastic constants of the mineral platelets and the organic matrix has been observed in biological materials. Young's modulus of the mineral platelets has been reported at the range of $50 \sim 205$ GPa, while the Young's modulus of the organic matrix varies a lot, e.g., $1 \sim 20$ MPa, or $15 \sim 20$ GPa.[32,45–48]

To investigate the effect of the contrast in Young's modulus on the evolution of CBGs, we focus on the Young's modulus of the organic matrix at the range of 20 MPa $\sim$ 2 GPa. Here we consider the unit cell with a lattice angle of 15° and the volume fraction and Young's modulus of the mineral platelets is set as 0.80 and 100 GPa, respectively. The evolution of CBGs as a function of modulus ratio between the mineral platelets and the organic matrix is reported in Fig. 8(a). The second CBG, which is the largest when the modulus of the organic matrix is 20 MPa, enlarges from 62.25 MHz to 71.50 MHz and then shrinks progressively towards closure as the modulus ratio decreases from 5000 to 50. Notably, other newly generated CBGs at smaller modulus ratio emerge at higher frequency range as the modulus ratio decreases. The largest width of CBGs appears when the modulus ratio decreases to intermediate values, indicating a proper selection of modulus ratio in the composites can help achieve the desired CBGs.

We then examine the effect of Poisson's ratio of the organic matrix on the evolution of CBGs. The Young's modulus of the organic matrix is set as 20 MPa and the Poisson's ratio is varied from 0.1 to 0.49.[47] The evolution of CBGs as a function of Poisson's ratio is given in Fig. 8(b). The width of the two CBGs shrinks steadily as the Poisson's ratio increases and both of the CBGs close as the organic matrix become nearly incompressible.

Although the volume fraction of the organic matrix is relative low in nacre-like composite, our study indicates that the contrast in elastic constants, i.e., Young's modulus and Poisson's ratio, and the compressibility of organic matrix are critical to the evolution of CBGs.

IV. CONCLUSION

We have numerically demonstrated the capability to manipulate the elastic wave propagation in bio-inspired periodic composites with nacre-like microstructure. Single or multiple CBGs are observed in the periodic composites with a wide range of lattice angles and volume fractions. The formation of these CBGs can be attributed to Bragg scattering or local resonances in each unit cell or due to both of them in the same periodic composites. Wide multiple CBGs can be obtained by utilizing these two formation mechanisms simultaneously. In addition, the investigation of elastic wave propagation in a finite periodic composite shows good agreement between transmission coefficient and the simulated CBGs, and further supports the origins of CBGs. The frequency tunability of CBGs can be achieved not only by engineering the lengthscale of the composites but also by tailoring the topological arrangement of the mineral platelets and material properties of each phase. The results of this work can help guide the creation of mechanically robust metamaterials while having integrated wave filtering property.

Note that here we only consider the first level of hierarchy of the nacre-like microstructure, while it has been observed that many biomaterials, e.g., nacre and bones, have multi-level structural hierarchy with self-similar microstructures.[33] This, in turn, gives rise to the formation of band gaps in broader frequency range on the transmission spectra of elastic wave propagation in one-dimensional periodic structure as compared to conventional periodic structures with single periodicity.[49] It is expected the hierarchy could also play a role to further improve CBGs and transmission spectrum of periodic composites with multi-level hierarchical nacre-like microstructures.

ACKNOWLEDGMENTS

The authors acknowledge the support of the National Science Foundation under Award number CMMI-1437449.

[1] M. Maldovan and E. L. Thomas, *Periodic Materials and Interference Lithography: For Photonics, Phononics and Mechanics* (John Wiley & Sons, 2009).
[2] J. H. Lee, J. P. Singer, and E. L. Thomas, Adv. Mater. **24**, 4782 (2012).
[3] M. Maldovan, Nature **503**, 209 (2013).
[4] R. Olsson III and I. El-Kady, Meas. Sci. Technol. **20**, 012002 (2009).
[5] M. S. Kushwaha, P. Halevi, L. Dobrzynski, and B. Djafarirouhani, Phys. Rev. Lett. **71**, 2022 (1993).
[6] M. Sigalas and E. N. Economou, Solid State Commun. **86**, 141 (1993).
[7] M. S. Kushwaha, Appl. Phys. Lett. **70**, 3218 (1997).
[8] A. Khelif, A. Choujaa, S. Benchabane, B. Djafari-Rouhani, and V. Laude, Appl. Phys. Lett. **84**, 4400 (2004).
[9] F.-L. Hsiao, A. Khelif, H. Moubchir, A. Choujaa, C.-C. Chen, and V. Laude, Phys. Rev. E **76**, 056601 (2007).
[10] J. Vasseur, A.-C. Hladky-Hennion, B. Djafari-Rouhani, F. Duval, B. Dubus, Y. Pennec, and P. Deymier, J. Appl. Phys. **101**, 114904 (2007).
[11] S. Gonella, A. C. To, and W. K. Liu, J. Mech. Phys. Solids **57**, 621 (2009).
[12] H. Lv, X. Tian, M. Y. Wang, and D. Li, Appl. Phys. Lett. **102**, 034103 (2013).
[13] K. Mikoshiba, J. M. Manimala, and C. T. Sun, J. Intell. Mater. Syst. Struct. **24**, 168 (2013).
[14] Z. Y. Liu, C. T. Chan, and P. Sheng, Phys. Rev. B **65**, 165116 (2002).
[15] Y. Achaoui, A. Khelif, S. Benchabane, L. Robert, and V. Laude, Phys. Rev. B **83**, 104201 (2011).
[16] M. M. Sigalas and E. N. Economou, J. Appl. Phys. **75**, 2845 (1994).
[17] C. Goffaux and J. Vigneron, Phys. Rev. B **64**, 075118 (2001).
[18] P. F. Hsieh, T. T. Wu, and J. H. Sun, Ieee Trans. Ultrason. Ferroelectr. Freq. Control **53**, 148 (2006).
[19] Y. Chen, H. Yao, and L. Wang, J. Appl. Phys. **114**, 043521 (2013).
[20] O. Sigmund and J. S. Jensen, Philos. Trans. R. Soc. London Seri. A- **361**, 1001 (2003).
[21] K. Bertoldi and M. Boyce, Phys. Rev. B **78**, 184107 (2008).
[22] L. F. Wang and K. Bertoldi, Int. J. Solids Struct. **49**, 2881 (2012).
[23] Z. Y. Liu, X. X. Zhang, Y. W. Mao, Y. Y. Zhu, Z. Y. Yang, C. T. Chan, and P. Sheng, Science **289**, 1734 (2000).
[24] C. Goffaux and J. Sánchez-Dehesa, Phys. Rev. B **67**, 144301 (2003).
[25] G. Wang, X. Wen, J. Wen, L. Shao, and Y. Liu, Phys. Rev. Lette. **93**, 154302 (2004).
[26] B. J. F. Bruet, J. H. Song, M. C. Boyce, and C. Ortiz, Nature Mater. **7**, 748 (2008).
[27] L. F. Wang, J. H. Song, C. Ortiz, and M. C. Boyce, J. Mater. Res. **24**, 3477 (2009).
[28] P. Y. Chen, A. Y. M. Lin, J. McKittrick, and M. A. Meyers, Acta Biomater. **4**, 587 (2008).
[29] M. A. Meyers, P. Y. Chen, A. Y. M. Lin, and Y. Seki, Progr. Mater. Sci. **53**, 1 (2008).
[30] J. C. Weaver, G. W. Milliron, A. Miserez, K. Evans-Lutterodt, S. Herrera, I. Gallana, W. J. Mershon, B. Swanson, P. Zavattieri, E. DiMasi, and D. Kisailus, Science **336**, 1275 (2012).
[31] X. D. Li, W. C. Chang, Y. J. Chao, R. Z. Wang, and M. Chang, Nano Lett. **4**, 613 (2004).
[32] F. Barthelat, C. M. Li, C. Comi, and H. D. Espinosa, J. Mater. Res. **21**, 1977 (2006).
[33] P. Fratzl and R. Weinkamer, Progr. Mater. Sci. **52**, 1263 (2007).
[34] M. A. Meyers, A. Y. M. Lin, P. Y. Chen, and J. Muyco, J. Mech. Behav. Biomed. Mater. **1**, 76 (2008).
[35] H. D. Espinosa, J. E. Rim, F. Barthelat, and M. J. Buehler, Progr. Mater. Sci. **54**, 1059 (2009).
[36] L. F. Wang and M. C. Boyce, Adv. Funct. Mater. **20**, 3025 (2010).
[37] A. Dutta, S. A. Tekalur, and M. Miklavcic, J. Mech. Phys. Solids **61**, 145 (2013).
[38] A. Khelif, B. Aoubiza, S. Mohammadi, A. Adibi, and V. Laude, Phys. Rev. E **74**, 046610 (2006).
[39] I. A. Aksay, M. Trau, S. Manne, I. Honma, N. Yao, L. Zhou, P. Fenter, P. M. Eisenberger, and S. M. Gruner, Science **273**, 892 (1996).
[40] F. D. Fleischli, M. Dietiker, C. Borgia, and R. Spolenak, Acta Biomater. **4**, 1694 (2008).
[41] H. D. Espinosa, A. L. Juster, F. J. Latourte, O. Y. Loh, D. Gregoire, and P. D. Zavattieri, Nature Commun. **2**, 173 (2011).
[42] A. Khelif, Y. Achaoui, S. Benchabane, V. Laude, and B. Aoubiza, Phys. Rev. B **81**, 214303 (2010).
[43] M. Kafesaki, M. M. Sigalas, and E. N. Economou, Solid State Commun. **96**, 285 (1995).
[44] E. N. Economou and M. Sigalas, J. Acoust. Soc. Am. **95**, 1734 (1994).
[45] R. Z. Wang, Z. Suo, A. G. Evans, N. Yao, and I. A. Aksay, J. Mater. Res. **16**, 2485 (2001).
[46] B. H. Ji and H. J. Gao, J. Mech. Phys. Solids **52**, 1963 (2004).
[47] S. Dashkovskiy, B. Suhr, K. Tushtev, and G. Grathwohl, Comput. Mater. Sci. **41**, 96 (2007).
[48] K. Bertoldi, D. Bigoni, and W. J. Drugan, Composites Sci. Technol. **68**, 1363 (2008).
[49] P. Zhang and A. C. To, Appl. Phys. Lett. **102**, 121910 (2013).